Static and dynamic density effects due to the finite length of polymer chains: a molecular-dynamics investigation

A Barbieri, D Prevosto, M Lucchesi and D Leporini §

Dipartimento di Fisica "Enrico Fermi", Università di Pisa, via F. Buonarroti 2, I-56127 Pisa, Italy

INFM Unità di Ricerca di Pisa

Abstract. The finite length of polymer chains affects both the static and the relaxation properties of the density of the melt state. These have been investigated by Molecular-Dynamics simulations of a Lennard-Jones model with fixed bond length. Under isothermal-isobaric conditions the density increases with the molecular weight. A suitable Voronoi tessellation reveals the extra free-volume around the chain ends and shows that it is strongly localized within the first end monomer. Simple arguments are given to interpret the main changes of the monomer radial distribution function and the corresponding static structure factor when the chain length is increased. As to the relaxation aspects of the density, it is found that the structural relaxation time increases with the molecular weight, which is interpreted as a signature of the well-known corresponding increase of the glass transition temperature.

Submitted to: *J. Phys.: Condens. Matter*

PACS numbers: 64.70.Pf, 61.25.Hq, 02.70.Ns

E-mail: `dino.leporini@df.unipi.it`

§ To whom correspondence should be addressed.

1. Introduction

The region surrounding the chain ends (CE) of polymer chains with finite length is characterized by imperfect ordering and packing [1]. Therefore, each CE possesses more free volume than if it were chemically bound within a continuous chain. Expectedly, this produces a plasticizing effect which enhances the mobility. The present paper aims at characterizing the changes of both the static and the fluctuation properties of the density when the relative fraction of CEs is changed, i.e. when the molecular weight M is changed.

Fox and Flory pioneered the study of the disorder introduced by the end groups of a linear chain (polystyrene) and evidenced by dilatometric measurements that the number density ρ depends on the number of monomers per chain M as [2]

$$\rho(M) = \left(\frac{1}{\rho_\infty} + \frac{2V_\mathrm{e}}{M} \right)^{-1} \tag{1}$$

where ρ_∞ is the number density in the limit of infinitely long chains and V_e is interpreted as the extra free-volume per CE. Fox and Flory also recognized that disrupting the local configurational order imparts an extramobility affecting the relaxation, and anticipated the well-known phenomenological relation between the glass transition temperature T_g and the chain length

$$T_\mathrm{g}(M) = T_{\mathrm{g}\infty} - \frac{C}{M} \tag{2}$$

where C is a positive constant and $T_{\mathrm{g}\infty}$ is the glass transition temperature in the limit of infinite length. The above equation was rationalized by assuming that the fractional free-volume $f(M)$ is nearly constant at the glass transition temperature T_g, $f(M) \simeq 1/40$, so that the free volume contributed by CEs have to be compensated by an additional thermal contraction [3, 4, 5, 6]. Even if it has been pointed out that that the glass is not a true iso-free-volume state [7], and improved expressions of the chain-length dependence of T_g have been derived by thermodynamic considerations [7, 8], the role played by the CEs in the polymer dynamics has been extensively studied over the years by several experiments [9, 10, 11, 12, 13, 14, 15, 16, 17, 18, 19, 20, 21, 22, 23, 24, 25], theoretical approaches [26, 27, 28] and numerical simulations [29, 30, 31, 32, 33, 34, 35, 36, 37, 38]. **Kremer and Grest first noticed by using a bead-spring model and studying the chain-length dependence of the statics and the dynamics that the terminal monomers exhibit faster dynamics than the central ones [29, 30]. More recent Monte Carlo studies also reached the same conclusions [31, 32].** Several issues have been addressed, including the effect of pressure on the relation between the glass-transition temperature and the molecular-weight of equation (2) [10], antiplasticization [13], the diffusion of small-molecule penetrants in polymers [14], the very interesting case of the dendrimers and hyperbranched polymers having an ever-increasing number of chain ends [9, 16, 20, 28], the interfacial dynamics of blends [11, 12, 21, 33] and thin polymer films [15, 22, 27], the diffusion in homopolymers and

blends [17, 18, 35, 36], the interaction energy between the free-volume and the polymer units [34], the rheology of food and biopolymers [23].

We present new results drawn by extensive classical molecular-dynamics (MD) simulations carried out on a melt of unentangled linear chains described by means of a Lennard-Jones model with fixed bond length, which captures the essential features of the chain-end influence. The model has been already extensively investigated over a wide temperature and pressure range to evidence scaling properties and the mutual role of the thermal and the density effects [47].

We profited from previous studies on the chain length dependence of the polymer dynamics [29, 30, 31, 32] and structure [39, 40, 41, 42, 43, 44, 45, 46].

As a novel issue we address explicitely the influence of the CEs free-volume on both the statics and the structural relaxation to investigate the microscopic origin of equation (2).

Remarkably, the efficient packing of the spherical beads limits the extra free-volume due to the CEs and gives insight into the sensitivity of the dynamics to this disorder effect. However, in more realistic models the packing of different polymer sites may be less efficient due to the poor interlocking of possible screening groups [41].

The paper is organized as follows. In section 2 the model and the numerical methods are detailed. In section 3 the results are presented and discussed. The conclusions are summarized in section 4.

2. Numerical Methods

We investigated systems of N linear chains with fixed bond length and M monomers (beads) each. The (M, N) pairs under investigation were $(3, 667)$, $(5, 200)$, $(7, 200)$, $(10, 200)$, $(15, 220)$, $(22, 300)$ and $(30, 300)$. The sample is confined into a cubic box with periodic boundary conditions. To handle the boundary conditions, the minimum image convention is adopted. The interaction between nonbonded monomers occurs via the Lennard-Jones (LJ) potential

$$U(r) = 4\epsilon \left[(\sigma/r)^{12} - (\sigma/r)^{6} \right] + U_{\rm cut} \tag{3}$$

The potential is cut off at $r_{\rm cut} = 2.5\sigma$ and properly shifted by $U_{\rm cut}$ so as to vanish at that point and to make it continuous everywhere.

Neighboring monomers in the same chain are constrained to a distance $b = 0.97\sigma$ by using the *RATTLE* algorithm [48]. From now on LJ units are adopted with the Boltzmann constant $k_{\rm B} = 1$. The samples are equilibrated under Nosé-Andersen [48] dynamics at the prescribed temperature and pressure until the average displacement of the chains' centers of mass is as large as twice the mean end-to-end distance. Data are collected during production runs in microcanonical conditions, by using a Verlet algorithm in velocity form. The time step is $\Delta t = 2.5 \times 10^{-3}$. No adjustment of the temperature, e.g. by rescaling the velocities, was needed during the production run.

The system is studied at pressure $P = 2.0$ and temperature $T = 1.2$. The results have been averaged over ten independent runs at least.

3. Results and discussion

3.1. Static effects

In figure 1 the dependence of the density on the chain length M is shown. It is fitted quite well by equation (1). V_e in equation (1) has to be interpreted as the extra free-volume around one CE with respect to that present around any other segment of the chain; the best-fit value is $V_e = 0.0905 \pm 0.0002$, i.e. about 17 % of the bead volume.

To characterize the structural disorder of the system we resorted to the Voronoi tessellation [49, 50]. Voronoi tessellation partitions the space into convex polyhedra. For a molecular system the Voronoi polyhedron is the region of space around an atom (in our case one bead), such that each point in this region is closer to the atom than to any other atom of the system. Figure 2 shows how the volume of the Voronoi polyhedra depends on the position of the bead along the chain. It is clearly seen that an excess volume is located at the CEs, whereas the polyhedra around all the other beads have almost identical volume. Excess volume around the CEs was also reported by atomistic simulations of polymers [35, 49, 50]. The present polymer model points out that, even if the packing of the beads is expectedly better than the one of more constrained atomistic structures (see e.g. [35, 49]), additional space is still found around the chain ends. We also see that flexible chains assign the extra free volume to the end monomers. An increased chain stiffness, on the other hand, distributes it also across adjacent monomers [35].

Since the average volume of the Voronoi polyhedra is by definition equal to the volume per particle, we may write

$$V_{\mathrm{inner}}(M) = \frac{1}{\rho(M)} - \frac{2\Delta V(M)}{M} \tag{4}$$

where $V_{\mathrm{inner}}(M)$ is the average volume of the polyhedra located around the inner monomers and $\Delta V(M)$ is the excess volume of the polyhedra located around CEs. By inspecting figure 2, $\Delta V(M)$ is found to be little dependent on M with average value $\Delta V = 0.0435 \pm 0.0015$. If the $M-$dependence of ΔV is neglected and equation (1) is replaced in equation (4), the latter yields a linear dependence of V_{inner} on M^{-1}. Indeed, the plot V_{inner} vs M^{-1} is remarkably linear (see the inset in figure 2) and the best-fit with equation (4), setting $\Delta V(M) = \Delta V^*$ and assuming (1), yields $\Delta V^* = 0.0436 \pm 0.0001$. Note that $\Delta V^* \neq V_e$, i.e. the excess free volume is different from the excess Voronoi volume. The difference is due to the fact that the available free volume around one tagged bead is also shared with the surrounding ones, and the boundary of the Voronoi polyhedron centered at the tagged bead cuts that free volume into two regions, one inside the polyhedron and the other outside. Since the bead volume is nearly constant, a small variation δV_{free} in the free volume leads to a variation $\delta V_{\mathrm{voronoi}}$ of the Voronoi

volume which should be slightly less than one half as small: $\delta V_{\rm voronoi} \sim (1-\epsilon)/2\ \delta V_{\rm free}$. The factor $\epsilon > 0$ depends on the detailed geometry and on the ratio between the Voronoi volume and the bead volume; we find $\epsilon \simeq 0.04$. Purely geometrical procedures in terms of Delauney tessellation to determine $V_{\rm e}$ are possible if the excess free volume $V_{\rm e}$ largely exceeds the free volume of the other monomers [35]. However, figure 2 suggests that this does not occur in the present study due to the good packing, and in this case possible corrections must also account for the softness of each bead due to the LJ interactions.

Figure 3 shows the radial distribution function $g_{\rm mon}(r)$ of the monomers without the delta-function contributions due to the bonded nearest-neighbours of each bead. It is seen that the maximum of $g_{\rm mon}(r)$ decreases with the chain length. No changes are observed beyond the first shell of nearest-neighbors. This is an interesting feature in that the density increases with the chain length (see figure 1) and one expects more short-range order. A simple argument shows that the decrease of the maximum follows from the different connectivity of the inner and end beads. Let us neglect the connectivity of the polymer chain with length M and consider the radial distribution function $g_{\rm LJ}(r)$ of the Lennard-Jones monoatomic liquid with the same average density. $g_{\rm LJ}(r)$ is conveniently calculated by using the Weeks-Chandler-Anderson theory (WCA) [51, 52, 53]. The average number of nearest-neighbours for the melt of chains with length M is given by:

$$N_{\rm mon}(M) = 4\pi\rho \int_0^{r_{\rm min}} dr\ r^2\ g_{\rm mon}(r) \tag{5}$$

$r_{\rm min}$ is the location of the first minimum of $g_{\rm mon}(r)$. Let $N_{LJ}(M)$ be the same quantity for the monoatomic Lennard-Jones liquid with the density of the melt of chains with length M, i.e. the analogue of equation (5) is written with $g_{\rm mon}(r)$ being replaced by $g_{\rm LJ}(r)$ which is integrated up to its first minimum. Figure 4 shows that $N_{\rm mon}(M)$ is virtually linear with $1/M$ and has a slope 2.42 whereas $N_{\rm LJ}(M)$, due to the small change of the density of the polymer melts with different chain lengths, is almost constant, $N_{\rm LJ}(M) \simeq 12$. $N_{\rm mon}(M)$ has two different terms. One, being ascribed to the inner beads, has weight $(M-2)/M$ and may be approximated by $N_{\rm LJ}(M)-2$ due to the missed contribution to $g_{\rm mon}(r)$ of the two bonded nearest-neighbours. A second terms with weight $2/M$ comes from the end beads and is approximated by $N_{\rm LJ}(M)-1$. Overall, $N_{\rm mon}(M)$ may be approximated by:

$$\tilde{N}(M) = N_{\rm LJ}(M) + \frac{2}{M} - 2 \tag{6}$$

$\tilde{N}(M)$ is compared to $N_{\rm mon}(M)$ in figure 4. The deviations do not exceed 15%. The slope of $\tilde{N}(M)$ vs. $1/M$ is about 2 to be compared with the slope 2.42 of $N_{\rm mon}(M)$.

Figure 3 also shows for all the investigated chain lengths the monomer

static structure factor $S_{\rm mon}(q)$ defined by the expression [53]

$$S_{\rm mon}(q) = 1 + 4\pi\rho \int_0^\infty [g_{\rm mon}(r) - 1] \frac{\sin(qr)}{qr} r^2 \, dr \tag{7}$$

It is seen that when the chain length increases the main peak of $S_{\rm mon}(q)$, S_{max}, located at q_{max} increases as well and shifts at higher q values . The changes become small at the highest investigated lengths. An approximate relation has been derived relating S_{max}, q_{max} and the width of the main peak Δq to be defined as the separation between the two adjacent nodes of $[S_{\rm mon}(q) - 1]$ embracing q_{max} [53]:

$$S_{max} \cong \frac{3q_{max}}{4\Delta q} (1 - \frac{6\pi^2\rho}{q_{max}^3}) \tag{8}$$

By considering $M = 3$ and $M = 30$ one finds $S_{max} = 2.21$ and $S_{max} = 2.24$ respectively to be compared with 2.2 and 2.26 from the simulation.

3.2. Relaxation effects

To characterize the relaxation dynamics of the density we evaluated the self-part of the intermediate scattering function:

$$F_{\rm s}(q,t) = \langle \exp[i\boldsymbol{q} \cdot (\boldsymbol{R}(t) - \boldsymbol{R}(0))] \rangle \tag{9}$$

where $\boldsymbol{R}(t)$ is the position of the monomer at time t and the brackets denote the suitable average over all the monomers. In figure 5 $F_{\rm s}(q,t)$ is plotted at $q_{\rm max}$ and $q_{\rm min}$, which are respectively the positions of the maximum and of the first minimum of $S_{\rm mon}(q)$. At late times the scattering functions $F_{\rm s}(q,t)$ exhibit a stretched-exponential decay with stretching parameters $0.7 \lesssim \beta \lesssim 0.75$, weakly decreasing with molecular weight. To characterize the decay of $F_{\rm s}(q,t)$, we define the structural relaxation time τ_α and $\tau_{\rm min}$ as the area below $F_{\rm s}(q_{\rm max},t)$ and $F_{\rm s}(q_{\rm min},t)$, respectively. The related integrals were evaluated numerically over the simulated time window. Both the quality of the data and the limited stretching made the above definition reliable.

The plots of τ_α and $\tau_{\rm min}$ versus the chain length are shown in figure 6. They both increase with the chain length. Being $q_{\rm min} > q_{\rm max}$, $\tau_{\rm min}$ is more affected by very local relaxation processes than τ_α. Then, it is not surprising that the former exhibits a weaker length dependence as it is shown in fig. 6.

The increase of the density-fluctuations time scales is consistent with the well-known increase of the glass transition temperature on increasing the polymer molecular weight, see equation (2) or the more complex expression provided by the entropy approach [7, 8]. Let us consider the usual Vogel-Fulcher law describing the temperature dependence of the relaxation times, i.e.

$$\tau(T) = A \exp\left(\frac{B}{T + C - T_{\rm g}}\right) \tag{10}$$

where A, B, C are constants. For simplicity, one neglects any molecular-weight dependence other than the one of T_g as given by equation (2). Far above the glass transition one finds

$$\tau(M) \simeq D \exp\left(-\frac{E}{M}\right) \tag{11}$$

where D, E depend only on the temperature.

Figure 6 shows that equation (11) accounts for the observed trends of both the structural relaxation time τ_α and $\tau_{\min}$ with the length of the chain. However, we are aware that deviations from equation (2) (on which equation (11) is based) are expected for short chains. Moreover, alternatives to equation (2) with more complicated M-dependence were found by the entropy approach [7, 8]. Overall, higher-quality data spanning a wider range of chain lengths are needed to assess the weight-dependence of the structural relaxation time.

4. Conclusions

We investigated the effects of finite length of polymeric chains in the melt state by MD simulation of Lennard-Jones model with fixed bond length. Both static and relaxation aspects were studied. It is found that under isothermal-isobaric conditions the density increases with the chain length according to equation (1). The Voronoi tessellation revealed the extra free-volume which is available around the chain ends. This extra volume is highly localized within the first end monomer. Simple arguments are given to interpret the main changes of the monomer radial distribution function and the corresponding static structure factor when the chain length is increased. As to the relaxation aspects of the density, it is found that the structural relaxation time increases with the molecular weight, which is interpreted as a signature of the well-known corresponding increase of the glass transition temperature.

Acknowledgments

Financial support from MIUR within the PRIN project "Dynamics and Thermodynamics in out-of-equilibrium materials: structural glasses, gels, polymeric materials" is gratefully acknowledged.

References

[1] Flory P J 1953 *Principles of Polymer Chemistry* (Ithaca: Cornell University Press)
[2] Fox T G and Flory P J 1950 *J. Appl. Phys.* **21** 581
[3] Bueche F 1962 *Physical Properties of Polymers* (New York: Interscience) chapters 3 and 4
[4] Bueche F and Kelley F N 1960 *J. Polym. Sci.* **45** 267
[5] Sperling L H 1992 *Introduction to Physical Polymer Science* 2nd edition (New York: Wiley)
[6] Ferry J D 1980 *Viscoelastic Properties of Polymers* 3rd edition (New York: Wiley)

[7] Gibbs J H and Di Marzio E A 1958 *J. Chem. Phys.* **28** 373
[8] Gedde U W 1995 *Polymer Physics* (London: Chapman and Hall)
[9] Wooley K L, Hawker C J, Pochan J M and Frechet J M J 1993 *Macromolecules* **26** 1514
[10] Toratani H and Takamizawa K 1994 *Polym. J.* **26** 797
[11] Cameron G G, Stewart D, Buscall R and Nemcek J 1994 *Polymer* **35** 3384
[12] Cameron G G, Qureshi M Y, Stewart D, Buscall R and Nemcek J 1995 *Polymer* **36** 3071
[13] Anderson S L, Grulke E A, Delassus P T, Smith P B, Kocher C W and Landes B G 1995 *Macromolecules* **28** 2944
[14] Hedenqvist M, Angelstok A, Edsberg L, Larsson P T and Gedde U W 1996 *Polymer* **37** 2887
[15] Tanaka K, Takahara A and Kajiyama T 1997 *Macromolecules* **30** 6626
[16] Farrington P J, Hawker C J, Frechet J M J and Mackay M E 1998 *Macromolecules* **31** 5043
[17] Von Meerwall E, Beckman S, Jang J and Mattice W L 1998 *J. Chem. Phys.* **108** 4299
[18] Von Meerwall E, Feick E J, Ozisik R and Mattice W L 1999 *J. Chem. Phys.* **111** 750
[19] Von Meerwall E, Ozisik R, Mattice W L and Pfister P M 2003 *J. Chem. Phys.* **118** 3867
[20] Morgan D R, Stejskal E O and Andrady A L 1999 *Macromolecules* **32** 1897
[21] Feldstein M M 2001 *Polymer* **42** 7719
[22] Jiang X Q, Yang C Z, Tanaka K, Takahara A and Kajiyama T 2001 *Phys. Lett. A* **281** 363
[23] Kasapis S 2001 *Food Hydrocolloids* **15** 631
[24] Capaccioli S, Casalini R, Lucchesi M, Lovicu G, Prevosto D, Pisignano D, Romano G and Rolla P A 2002 *J. non Cryst. Solids* **307-310** 238
[25] Prevosto D, Capaccioli S, Lucchesi M and Rolla P A in press on *Macromolecular Symposia.*
[26] Matsuoka S and Hale A 1997 *J. Appl. Polym. Sci.* **64** 77
[27] DeGennes P G 2000 *Eur. Phys. J. E* **2** 201
[28] Liu H W, Wilen C E and Shi W F 2002 *Macromol. Theor. Simul.* **11** 459
[29] Grest G S and Kremer K 1986 *Phys. Rev. A* **33** 3628
[30] Grest G S and Kremer K 1990 *J. Chem. Phys.* **92** 5087
[31] Binder K and Paul W 1997 *J.Polym.Sci: PartB:Polymer Phys.* **35** 1
[32] Paul W 2002 *Chem.Phys.* **284** 59
[33] Muller M, Binder K and Oed W 1995 *J. Chem. Soc. Farad. Trans.* **91** 2369
[34] Rane S and Gujrati P D 2001 *Phys. Rev. E* **64** 011801
[35] Harmandaris V A, Doxastakis M, Mavrantzas V G and Theodorou D N 2002 *J. Chem. Phys.* **116** 436
[36] Harmandaris V A, Angelopoulou D, Mavrantzas V G and Theodorou D N 2002 *J. Chem. Phys.* **116** 7656
[37] Harmandaris V A, Mavrantzas V G and Theodorou D N 1998 *Macromolecules* **31** 7934
[38] Harmandaris V A, Mavrantzas V G, Theodorou D N, Kröger M, Ramirez J, Ottinger H C and Vlassopoulos D 2003 *Macromolecules* **36** 1376
[39] Schweitzer K S and Curro J G 1997 *Adv.Chem.Phys.* **98** 1
[40] Curro J G, Schweitzer K S, Grest G S and Kremer K 1989 *J. Chem. Phys.* **91** 1357
[41] Weinhold J D, Curro J G, Habenschuss A and Londono J D 1999 *Macromolecules* **32** 7276
[42] Pütz M, Curro J G and Grest G S 2001 *J. Chem. Phys.* **114** 2847
[43] Sides S W, Curro J G, Grest G S, Stevens M J, Soddemann T, Habenschuss A and Londono J D 2002 *Macromolecules* **35** 6455
[44] Yethiraj A, Hall C K and Honnell K G 1990 *J. Chem. Phys.* **93** 4453
[45] Yethiraj A and Hall C K 1992 *J. Chem. Phys.* **96** 797
[46] Aichele A, Chong S H, Baschnagel J and Fuchs M 2004 *Phys.Rev.E* **69** 061801
[47] Barbieri A, Capaccioli S, Campani E and Leporini D 2004 *J. Chem. Phys.* **120** 437
[48] Allen M P and Tildesley D J 1987 *Computer Simulation of Liquids* (Oxford: Clarendon Press)
[49] Rigby D and Roe R J 1990 *Macromolecules* **23** 5312
[50] Tokita N, Hirabayashi M, Azuma C and Dotera T 2004 *J. Chem. Phys.* **120** 496
[51] Andersen H C, Chandler D and Weeks J D 1976 *Adv.Chem.Phys.* **34** 105

[52] Verlet L and Weis J-J 1972 *Phys. Rev. A* **5** 939
[53] March N H, Tosi M P 2002 *Introduction to Liquid State Physics* (Singapore: World Scientific Publishing Co.)

Figure captions

Figure 1. The dependence of the density on the molecular weight M. The superimposed curve is the fit with equation (1) with $\rho_\infty = 0.961 \pm 0.002$ and $V_e = 0.0905 \pm 0.0002$.

Figure 2. The average volume of the Voronoi polyhedron around the bead located at n position along the chain (symmetric positions with respect to the center of the chain are averaged over: $n \leq M/2$). Note the larger volume of the polyhedra surrounding the CEs ($n = 1$). The average excess volume is $\Delta V = 0.0435 \pm 0.0015$. Inset: Chain-length dependence of the Voronoi volume of the inner beads $V_{\rm inner}$. The superimposed curve is equation (4) with $\Delta V(M) = \Delta V^*$. The best fit value is $\Delta V^* = 0.0436 \pm 0.0001$.

Figure 3. Radial distribution function $g_{\rm mon}(r)$ of the monomers (top) and static structure factor $S_{\rm mon}(q)$ (bottom) for all the investigated chain lengths. The insets show a detailed view of the maxima of $g_{\rm mon}(r)$ (top) and $S_{\rm mon}(q)$ (bottom). Symbols refer to: $M = 3$ (circles), 5 (squares), 15 (diamonds), 30 (triangles). By increasing the chain length the maximum of $g_{\rm mon}(r)$ decreases whereas the maximum of $S_{\rm mon}(q)$ increases and shifts to higher q-values. See text for details.

Figure 4. Chain-length dependence of the number of nearest-neighbours monomers $N_{\rm mon}(M)$ (equation (5)) from MD simulations (filled circles). The number of nearest-neighbours atoms $N_{\rm LJ}(M)$ for the Lennard-Jones monoatomic liquid with the same density of the polymer melt with chain length M is also shown (empty squares) together with the approximation $\tilde{N}(M)$ (equation (6)) (empty circles). The slopes of $N_{\rm mon}(M)$ and $\tilde{N}(M)$ are about 2.4 and 2.0, respectively. See text for details.

Figure 5. Plot of the self-part of the intermediate scattering function F_s at $q = q_{\rm max}$ (shaded symbols) and $q = q_{\rm min}$ (open symbols). Inset: plot of $-\ln[F_s]$ at the same values of q.

Figure 6. Molecular weight dependence of the structural relaxation time τ_α (circles) and $\tau_{\rm min}$ (squares). The superimposed curves are fits with equation (11); the fit parameters are $D_\alpha = 0.70$, $D_{\rm min} = 0.30$, $E_\alpha = 1.08$, $E_{\rm min} = 0.87$.

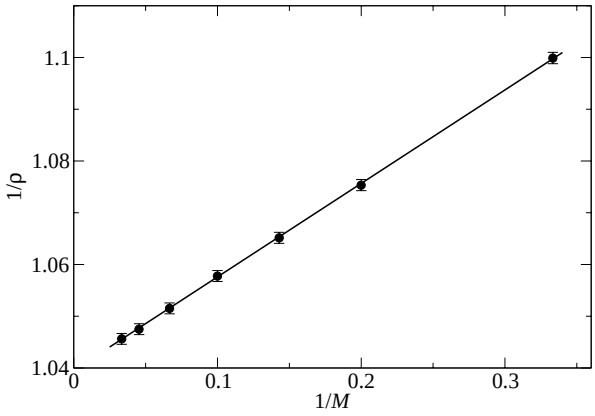

FIGURE 1

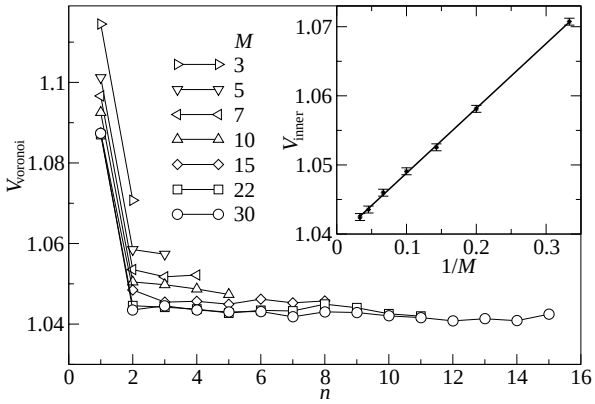
M
3
5
7
10
15
22
30
$V_{voronoi}$
1.1
1.08
1.06
1.04
0
2
4
6
8
10
12
14
16
n
V_{inner}
1.07
1.06
1.05
1.04
0
0.1
0.2
0.3
1/M

FIGURE 2

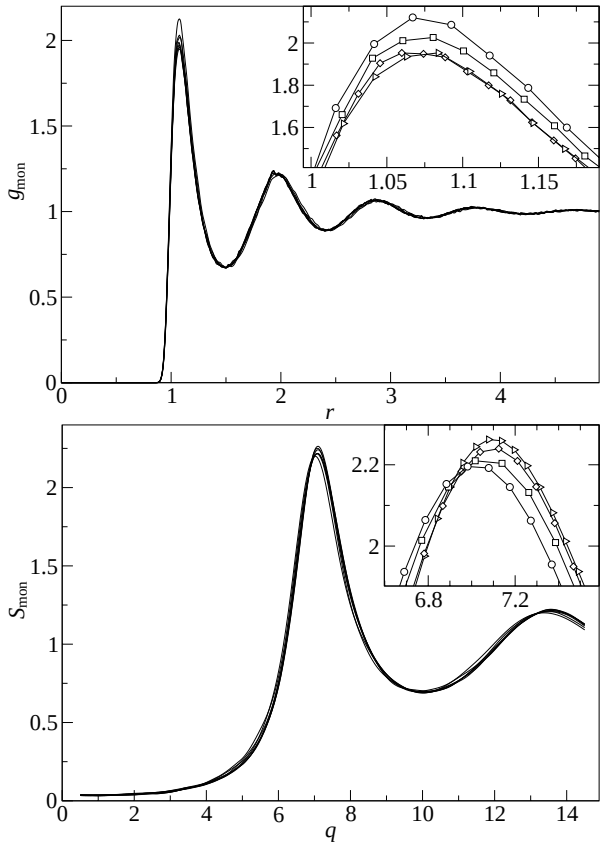

FIGURE 3

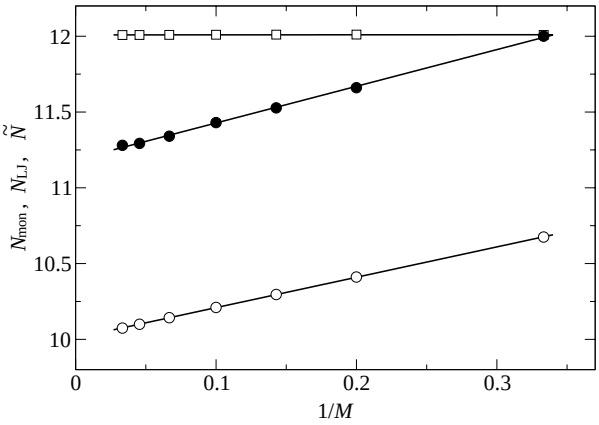

FIGURE 4

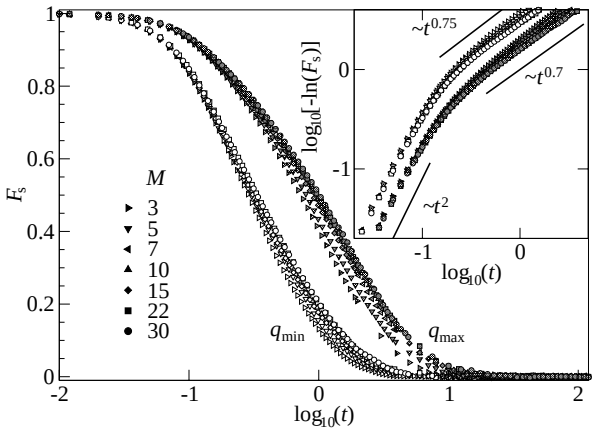
F_s
$\log_{10}(t)$
M
3
5
7
10
15
22
30
q_{min}
q_{max}
$\log_{10}[-\ln(F_s)]$
$\sim t^{0.75}$
$\sim t^{0.7}$
$\sim t^2$

FIGURE 5

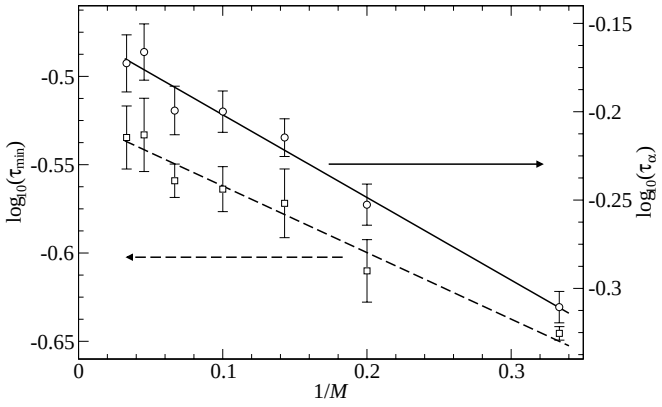

FIGURE 6